UC Irvine
UC Irvine Previously Published Works

Title

Cardiovascular Function and Structure are Preserved Despite Induced Ablation of BMP1-Related Proteinases

Permalink

https://escholarship.org/uc/item/18n160qr

Journal

Cellular and Molecular Bioengineering, 11(4)

ISSN

1865-5025

Authors

Golob, Mark J
Massoudi, Dawiyat
Tabima, Diana M
et al.

Publication Date

2018-08-01

DOI

10.1007/s12195-018-0534-y

Peer reviewed

BMES
BIOMEDICAL ENGINEERING SOCIETY™
www.bmes.org

CrossMark

Cardiovascular Function and Structure are Preserved Despite Induced Ablation of BMP1-Related Proteinases

Mark J. Golob,[1] Dawiyat Massoudi,[2] Diana M. Tabima,[1] James L. Johnston,[1] Gregory D. Wolf,[1] Timothy A. Hacker,[3] Daniel S. Greenspan,[2] and Naomi C. Chesler[1,3]

[1]Department of Biomedical Engineering, University of Wisconsin-Madison College of Engineering, Madison, WI 53706, USA; [2]Department of Cell and Regenerative Biology, University of Wisconsin-Madison School of Medicine and Public Health, Madison, WI 53706, USA; and [3]Department of Medicine, University of Wisconsin School of Medicine and Public Health, Madison, WI 53706, USA

Abstract

Introduction—Bone morphogenetic protein 1 (BMP1) is part of an extracellular metalloproteinase family that biosynthetically processes procollagen molecules. BMP1-and tolloid-like (TLL1) proteinases mediate the cleavage of carboxyl peptides from procollagen molecules, which is a crucial step in fibrillar collagen synthesis. Ablating the genes that encode BMP1-related proteinases (*Bmp1* and *Tll1*) post-natally results in brittle bones, periodontal defects, and thin skin in conditional knockout (BT^{KO}) mice. Despite the importance of collagen to cardiovascular tissues and the adverse effects of *Bmp1* and *Tll1* ablation in other tissues, the impact of *Bmp1* and *Tll1* ablation on cardiovascular performance is unknown. Here, we investigated the role of *Bmp1*- and *Tll1*-ablation in cardiovascular tissues by examining ventricular and vascular structure and function in BT^{KO} mice.
Methods—Ventricular and vascular structure and function were comprehensively quantified in BT^{KO} mice ($n = 9$) and in age- and sex-matched controls ($n = 9$). Echocardiography, cardiac catheterization, and biaxial *ex vivo* arterial mechanical testing were performed to assess tissue function, and histological staining was used to measure collagen protein content.
Results—*Bmp1*- and *Tll1*-ablation resulted in maintained hemodynamics and cardiovascular function, preserved biaxial arterial compliance, and comparable ventricular and vascular collagen protein content.
Conclusions—Maintained ventricular and vascular structure and function despite post-natal ablation of *Bmp1* and *Tll1* suggests that there is an as-yet unidentified compensatory mechanism in cardiovascular tissues. In addition, these findings suggest that proteinases derived from *Bmp1* and

Tll1 post-natally have less of an impact on cardiovascular tissues compared to skeletal, periodontal, and dermal tissues.

INTRODUCTION

Members of a small family of structurally-similar extracellular metalloproteinases, including bone morphogenetic protein 1 (BMP1), mammalian tolloid (mTLD), and tolloid-like 1 and 2 (TLL1, TLL2), are broadly expressed in tissues and have roles in processing procollagen molecules and other precursors of various extracellular matrix (ECM) components.[34,44] These BMP1/tolloid-related proteinases (BTPs) affect a crucial step in fibrillar collagen synthesis: cleavage of the carboxyl propeptide domain from procollagen molecules.[19,25] The genes that encode these proteinases (*Bmp1* for BMP1 and mTLD; *Tll1* for TLL1) have been individually knocked out in mice to investigate the role of BTPs in tissues with abundant collagen. Mice homozygous null for the *Bmp1* gene were perinatal lethal while those null for the *Tll1* gene were embryonic lethal due to cardiovascular defects.[8,41] To prevent early mortality and allow postnatal study of BTP-ablation, mice conditionally null for both *Bmp1* and *Tll1* were created. These mice are referred to as BT^{KO} mice. BT^{KO} mice treated with tamoxifen at 4 and 5 weeks of age to induce the conditional knockout have brittle bones with spontaneous fractures, periodontal defects, thin skin, and reduced processing of procollagen in these tissues at approximately 18 weeks of age.[33,34,52] Results from these studies indicate that

proteinases derived from *Bmp1* and *Tll1* strongly impact skeletal, periodontal, and dermal tissue function and structure and are implicated in disease.

Cardiovascular tissues contain mostly fibrillar collagen types I and III, which comprise approximately 25–55% of the ECM.[35] Collagen has integral roles in the cardiovascular system including interconnecting cardiac cells, contributing to arterial and valvular mechanical properties, and preventing excessive arterial deformation at high pressures. Changes in collagen accumulation and cross-linking are important to tissue remodeling processes in healthy and diseased states.[3,17,31] Disruption of the balance between collagen synthesis and degradation has been linked to cardiovascular disease and ventricular dysfunction.[3,9,39] Specifically with age and hypertension, collagen accumulation contributes to arterial stiffening leading to increased ventricular afterload, causing further stiffening in a positive feedback loop.[10,36,47,49]

Despite the importance of collagen types I and III to cardiovascular function and the adverse effects of 14 weeks of *Bmp1* and *Tll1* ablation in skeletal, periodontal, and dermal tissues in adult mice, the consequences of *Bmp1* and *Tll1* ablation on cardiovascular structure and function have not yet been studied. Here, we investigated the role of BTP-ablation in cardiovascular tissues by examining ventricular and vascular structure and function in BT^KO mice. We measured cardiovascular function in adult BT^KO mice after 14 weeks of *Bmp1* and *Tll1* ablation for consistency with previous studies that found significant defects in other tissues with identical treatment.[33,34] Echocardiography, cardiac catheterization, and biaxial *ex vivo* arterial mechanical testing were performed to assess tissue function, and histological staining was used to measure collagen protein content. Metrics of ventricular and vascular structure and function were maintained in BT^KO mice. Our results indicate that cardiovascular structure and function were preserved despite induced BTP-ablation.

MATERIALS AND METHODS

Animals

Male and female BT^KO mice ($n = 9$) were generated as described previously.[34] Briefly, mice carrying the Cre transgene, under the control of the ubiquitin C promoter, were crossed with mice with a $Bmp1^{flox/flox}$; $Tll1^{flox/flox}$ background to produce BT^KO mice ($Bmp1^{flox/flox}$; $Tll1^{flox/flox}$; Cre). To ensure a global knockout, the Cre trans *Bmp1* and *Tll1* sequences in Cre-expressing mice were excised through administration of tamoxifen (Sigma, Life Science) via IP injection

at a concentration of 100 mg/kg body weight once per day for five days at 4 weeks of age and again for 5 days at 5 weeks of age. Male and female littermates lacking the Cre transgene ($Bmp1^{flox/flox}$; $Tll1^{flox/flox}$) were used as controls ($n = 9$), and tamoxifen was also administered. Body weight (BW) was measured weekly. The gene excision efficiency was measured by PCR using genomic DNA from ear punch samples at ~ 12 weeks of age, and mice were only included in analyses if the gene excision efficiency was greater than 70%. Ventricular function and arterial mechanics were tested at approximately 18 weeks of age for consistency with the age of mice and duration of *Bmp1* and *Tll1* ablation with prior studies.[33,34] The University of Wisconsin-Madison Institutional Animal Care and Use Committee approved all procedures.

Echocardiography

Non-invasive metrics of cardiopulmonary function were measured using echocardiography procedures as previously described[5] at 10, 14, and approximately 18 weeks of age, which correspond to 6, 10, and 14 weeks, respectively, after tamoxifen treatment to activate the transgene. Measurements were made at these time points to examine whether adverse cardiovascular events were evident at or before the duration of *Bmp1* and *Tll1* ablation where defects were previously observed in other tissues. Measurements were performed on an additional ten female mice ($n = 5$ controls; $n = 5$ BT^KO) at 26, 30, and 34 weeks of age to examine whether adverse phenotypes would occur with longer durations of *Bmp1* and *Tll1* ablation. Briefly, mice were anesthetized with isoflurane (1%) while body temperature was maintained at 37 °C using a heated pad. A 30-MHz transducer (RMV 707B, Visual Sonics, Toronto) was used to obtain 2D guided M-mode and Doppler images in the left and right ventricles (LV and RV, respectively). RV wall thickness, mitral (MVE, MVA) and tricuspid (TVE, TVA) valve velocities in early and late diastole, fractional shortening (FS), and aorta (Ao) and pulmonary artery (PA) diameters and ejection times (ET) were determined from images acquired over at least three consecutive heartbeats. LV wall thickness was estimated using LV dimensions in diastole as previously reported.[5]

Cardiac Catheterization

Surgical preparation and catheterization procedures were based on established protocols.[30,43] Anesthesia was induced via urethane (1.8–2 mg/g BW) to maintain heart rate, and mice were intubated and placed on

a ventilator (Harvard Apparatus, Holliston, MA). Systemic blood pressures and heart rate (HR) were continuously recorded using a pressure catheter (Millar, Houston, TX) placed in the aortic arch. Pressure–volume loops for the LV and then RV were obtained using a 1.2 F, 3.5 mm spaced, admittance catheter (Scisense, London, Ontario, Canada) with software (Notocord, Croissy Sur Seine, France) recording waveforms at 1 kHz. Ventricular function was quantified using established metrics including end-systolic pressures, relaxation time (τ), ejection fraction (EF), maximum and minimum pressure derivatives (dP/dt_{max}, dP/dt_{min}), cardiac index (CI; cardiac output/body weight) stroke volume index (SVI; stroke volume/body weight), arterial elastance (E_a), stroke work (SW), ventricular compliance, and total vascular resistance (TVR).

Hematocrit, Tissue Weights, and Tibia Length

Following cardiac catheterization, animals were euthanized, and a blood sample was immediately centrifuged to measure hematocrit (Hct). The atria, ventricles, and lung lobes were weighed, and tibia length was measured (TL).

Ex Vivo Biaxial Mechanical Testing

The descending thoracic aortas (DTA) were harvested and tested using a modified version of the isolated vessel mechanical testing system previously used in our group.[22,29,51] To measure axial force during vessel extension, a force transducer (400A, Aurora Scientific) was added to the system and affixed to a 3-stage micrometer (Parker, Hannifin Corporation, Mayfield Heights, OH) for three dimensional control of the distal cannula. Preliminary tests on aortas from C57BL6 mice demonstrated a nonlinear axial force response to axial stretch as expected from the literature.[18]

The DTA was submerged in PBS, cannulated, affixed to the cannulas using suture ties, and the suture–suture length was measured. The approximate *in vivo* axial stretch (λ_{iv}) was experimentally determined by increasing the pressure at a fixed axial stretch until the force response was constant.[20,48] The DTA was then stretched to λ_{iv}, equilibrated at 90 mmHg for at least 30 min and preconditioned with at least three sinusoidal cycles at 0.014 Hz from 10 to 140 mmHg.[29] Vessel outer diameter (OD) was measured at 5 mmHg to approximate the no-load state. Static inflation testing for the circumferential direction was performed by measuring OD from 10 to 140 mmHg with 10 mmHg increments for at least 30 s at each step. Axial preconditioning was performed 3 times from $\lambda = 1$ to λ_{iv}

at a rate of ~ 10 μm/s.[1] Static extension testing for the axial direction was then performed at 90 mmHg by measuring axial force (F) at multiple axial stretch values in increments of 0.1. Finally, dynamic testing was performed at λ_{iv} to quantify viscoelastic properties at physiologically relevant frequencies as done previously.[22,51] Sinusoidal pressure waveforms from 90 to 120 mmHg at 1, 5, and 10 Hz were applied to each vessel.

Analysis of Ex Vivo Arterial Mechanical Properties

The circumferential stretch ratio (λ_θ) was calculated using the diameter measured at each pressure (OD_p) and the reference diameter at 5 mmHg (OD_5).

$$\lambda_\theta = \frac{OD_p}{OD_5} \tag{1}$$

The axial stretch ratio (λ_z) was calculated using the stretched length (l_L) and the suture–suture length (l_o).

$$\lambda_z = \frac{l_L}{l_o} \tag{2}$$

Wall thickness (h) was calculated as a function of pressure[14,36] using the outer diameter (OD) and wall thickness at the maximum pressure (OD_{max} and h_{max}).[14,36]

$$h = \frac{1}{2}\left[OD_p - \sqrt{OD_p^2 - OD_{max}^2 + (OD_{max} - 2h_{max})^2}\right] \tag{3}$$

This analysis assumes arteries are homogenous and incompressible, and the software tracks the arterial wall using an algorithm that automatically detects differences in pixel intensity between the arterial wall and the lighter lumen and background. Experimental 2nd Piola–Kirchhoff stresses in the circumferential (S_θ) and axial (S_z) directions were calculated using the applied pressure (P), axial force (F), DTA inner radius (r_i), and DTA outer radius (r_o).

$$S_\theta = \frac{Pr_i}{h\lambda_\theta^2} \tag{4}$$

$$S_z = \frac{F + P\pi r_i^2}{\pi(r_o^2 - r_i^2)\lambda_z^2} \tag{5}$$

Green strain (E) was calculated using the stretch in each direction (θ = circumferential; z = axial).

$$E_i = \frac{1}{2}(\lambda_i^2 - 1); \quad i = \theta, z \tag{6}$$

Linear regression lines were fit to the total strain range, low-, and high-strain regions of the S–E curve

(Fig. 1) to determine overall, low-, and high-strain moduli as previously done by our group.[21,28,42,49] Transition strain was taken as the intersection of the lines of best fit for the low- and high-strain regions (Fig. 1). An extrinsic property, structural stiffness, was determined in the circumferential and axial directions from the slope of the pressure-circumferential stretch and force-axial stretch relationships, respectively. Arteries exhibit viscoelastic characteristics, so we calculated a dynamic modulus and arterial damping at each testing frequency as previously done.[22,53] Briefly, the dynamic elastic modulus was calculated as the slope of the best fit line to the stress–strain hysteresis loop generated by loading and unloading cycles. The energy loss during a pressure cycle, the arterial damping, was calculated as the ratio of dissipated to stored energy from the resulting hysteresis loop. All mechanical properties were calculated using a custom routine in MATLAB R2016a (Mathworks, Natick, MA).

Histology

DTA and LV tissues were fixed in 10% formalin, preserved in 70% ethanol, embedded in paraffin, and then sectioned. Picrosirius red and Verhoeff van Gieson stains were used to measure the ECM proteins collagen and elastin, respectively. An inverted microscope (TE-2000-5, Nikon, Melville, NY) connected to a Spot CCD camera (Optical Analysis Systems, Nashua, NH) was used for image acquisition. The area containing ECM proteins was determined using color thresholding schemes in representative fields of view by an observer blinded to the experimental condition.[23,50] Percentage of ECM proteins was calculated by dividing area marked positive for ECM proteins by the total tissue area. Collagen types I and III, which are major constituents in cardiovascular tissues, were measured using polarized light with a yellow/orange and green thresholding scheme as previously done in our group.[21] We report collagen content as the sum of type I and type III collagen values from the same sample.

Primary Cardiac Fibroblast Culture

Harvesting and culturing of primary cardiac fibroblasts were conducted as previously described.[27] For immunoblotting, cells were grown to 80–90% confluence. Cells were then washed three times with PBS to remove residual FBS before being serum starved in DMEM supplemented with 10 μg/mL TGFβ (R&D), 100 μg/mL L-ascorbic acid (Sigma), and 40 μg/mL soybean trypsin inhibitor (Sigma).

Twenty-four hours post starvation conditioned media samples were collected and concentrated by centrifugation filters (Millipore).

Western Blot

Concentrated conditioned cardiac fibroblast media samples were used for immunoblotting. For probiglycan and biglycan immunoblotting, samples were treated with 2.5 mU Chondroitinase ABC (Sigma) at 37 °C for 4 h prior to immunoblotting. All samples were subjected to SDS-PAGE, and then transferred to nitrocellulose membranes, which were then blocked in 5% nonfat dry milk supplemented with 1% BSA. Blots were probed with anti-α1(I) (LF-68), anti-pro-α1(I) C-propeptide (LF-41), anti-probiglycan (LF-104), and anti-biglycan (LF-159)[16]; all diluted 1:1000. Secondary antibodies used were IR800 conjugated anti-rabbit IgG (Li-Cor) diluted 1:15000. Blots were visualized using an Odyssey FC Imager (Li-Cor). All immunoblots were repeated using 3 different BT^{KO} and control samples.

Statistics

Data are reported as mean ± standard error. Comparisons between control and BT^{KO} tissues were conducted using a student's *t* test with a two-sided *p*-value < 0.05 to indicate statistical significance. A repeated measures ANOVA was used for echocardiography data at each time point. Model assumptions for analyses were validated by examining normal probability plots. Tukey's Honestly Significance Difference method was utilized to control the type I error when conducting multiple comparisons. All analyses were conducted using R-software version 3.2.2 (R, Foundation for Statistical Computing, USA) unless otherwise specified.

RESULTS

Bmp1/Tll1 Ablation and Reduced Procollagen Processing

PCR analysis of control and BT^{KO} cardiac genomic DNA showed excision of *Bmp1* (Fig. 2a). Western blotting showed reduced procollagen I C-propeptide cleavage by cardiac fibroblasts of BT^{KO} mice, as evidenced by higher levels of procollagen and pCα1(I) chains (a processing-intermediate that retains the C propeptide) and reduced amounts of free C-propeptide (Fig. 2b). There was also reduced cleavage of probiglycan into mature biglycan (Fig. 2c), another ECM component cleaved by BTPs.[40]
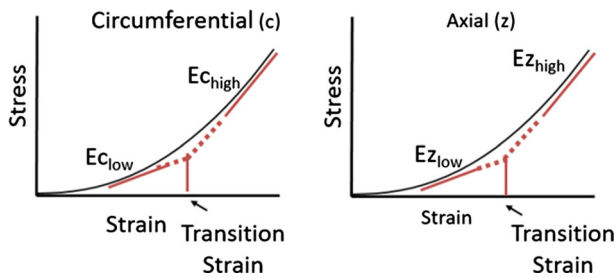
FIGURE 1. Stress-strain curves illustrating how the low- and high-strain moduli and transition strain were calculated for data obtained based on circumferential and axial testing protocols. Ec_{low} = circumferential low-strain modulus; Ec_{high} = circumferential high-strain modulus; Ez_{low} = axial low-strain modulus; Ez_{high} = axial high-strain modulus.
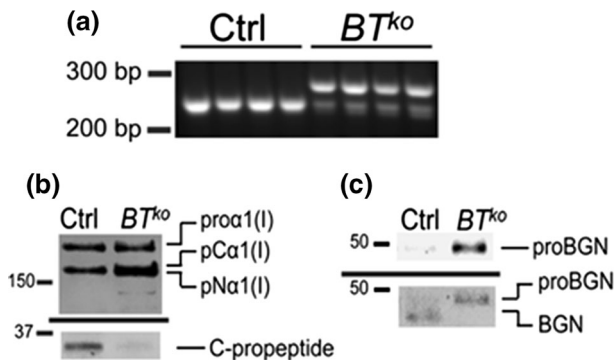
FIGURE 2. (a) Excision of *Bmp1* in BT^{KO} mice. (b) Western blots, employing antibodies to the $\alpha1(I)$ chain C-telopeptide (top blot) or C-propeptide (bottom blot), showing reduced processing of procollagen (processing intermediates pC and pN retain the C and N propeptides, respectively). There are increased levels of pC$\alpha1(I)$ and reduced levels of free C-propeptides in the BT^{KO} sample. (c) Western blots, employing antibodies specific to uncleaved pro-biglycan (top blot), or an antibody that recognizes both pro- and mature biglycan (bottom blot) showing reduced processing of pro-biglycan and lower levels of mature biglycan in the BT^{KO} sample.

Body Weight, Hematocrit, Tibia Length, and Tissue Weights

BT^{KO} mice had reduced weight gain with time compared with control mice as reported previously.[34] Differences were statistically significant starting at 13 weeks of age (Fig. 3a). The reduced weight gains in the BT^{KO} mice continued in ten additional female mice observed out to 34 weeks of age (Fig. S1). At the terminal time point of ~ 18 weeks, the reduction in total heart weight was proportional to the reduction in body weight (Figs. 3b and 3c). Tibia length was smaller in BT^{KO} mice (Fig. 3d). Only LV + S and lung weight normalized to BW were significantly larger in BT^{KO} mice (Table S1).

Hemodynamics and Cardiovascular Function

Systemic pressures and metrics of LV and RV function were preserved in BT^{KO} mice at ~ 18 weeks of age (Tables 1, S2, S3). We investigated if adverse phenotypes would be evident with age, but we found that functional metrics were still preserved up to 34 weeks of age in females (Table S4).

Arterial Mechanics

The approximate *in vivo* axial stretch was experimentally determined to be 1.54 ± 0.03 for control and 1.48 ± 0.02 for BT^{KO} mice ($p = 0.163$). Using the experimentally determined physiological pressure range from catheterization (30–70 mmHg; Table 1), biaxial arterial compliance was preserved in BT^{KO} mice as measured by elastic moduli and structural stiffness in the circumferential and axial directions (Fig. 4 and Tables 2, S5). Based on heart rates measured from catheterization (Table 1), dynamic properties were calculated at an approximate physiological frequency of 10 Hz. Dynamic modulus and arterial damping were not different between the groups at physiological or sub-physiological frequencies (Table S5).

Extracellular Matrix Content

Collagen content was assessed in the LV and DTA, and elastin was assessed in the DTA. Collagen and elastin content are expressed as a tissue area percentage in the vessel wall from color thresholding. Collagen and elastin content were comparable between the two groups in the DTA (Figs. 6a and 6b; collagen: $p = 0.700$; elastin: $p = 0.428$). Similarly, perivascular fibrosis as measured by LV collagen content was comparable between control and BT^{KO} mice (Fig. 6c; $p = 0.285$).

DISCUSSION

Based on the importance of fibrillar collagens to cardiovascular tissue function and the adverse effects of *Bmp1*- and *Tll1* knockdown in skeletal, periodontal, and dermal tissues, we investigated the impact of *Bmp1* and *Tll1* ablation in cardiovascular tissues. We found that *Bmp1* and *Tll1* ablation resulted in maintained hemodynamics and cardiovascular function (Tables 1, S2–S4), preserved biaxial arterial compliance (Fig. 4 and Tables 2, S5), and comparable ventricular and vascular ECM protein content (Fig. 6). The reduction in absolute heart weight was proportional to the reduced body weight, indicating that there was not a
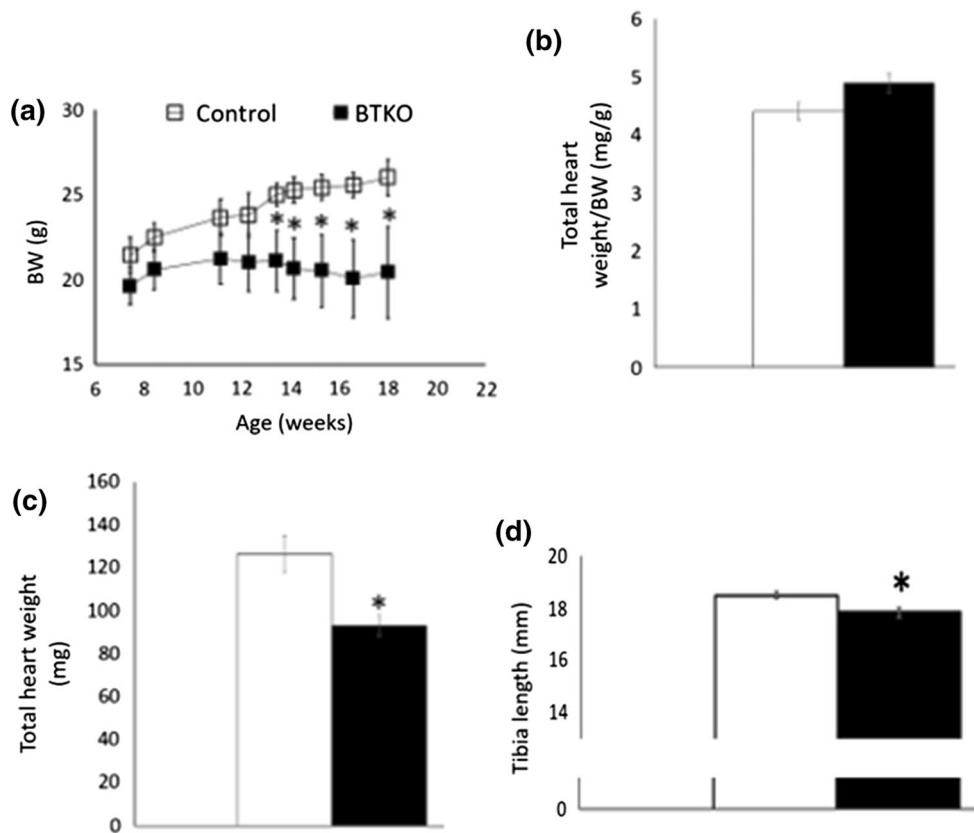
FIGURE 3. (a) BT^{KO} mice (black squares) had reduced weight gain over time compared to control mice (white squares). Differences in BW were statistically significant starting at 13 weeks old. (b) Total heart weight was reduced in the BT^{KO} mice (black bar) compared with controls (white bar; $p = 0.006$), but (c) the total heart weight normalized to body weight was not significantly different between the two groups ($p = 0.052$, indicating the reduction in cardiac muscle mass was proportional to the reduced body weight. (d) Tibia length was reduced in BT^{KO} mice ($p = 0.012$). *$p < 0.05$ vs. control. Sample size = 18.

TABLE 1. Hemodynamic and ventricular function measurements for control and BT^{KO} mice.

	Control	BT^{KO}	p-value
Systemic pressure			
Systolic (mmHg)	67 ± 6	60 ± 2	0.319
Diastolic (mmHg)	39 ± 5	33 ± 2	0.285
Pulse (mmHg)	27 ± 2	27 ± 1	0.946
LV and systemic circulation			
Systolic pressure (mmHg)	49 ± 4	46 ± 4	0.514
τ (ms)	7 ± 1	9 ± 1	0.167
EF (%)	54 ± 4	52 ± 6	0.776
CI (μL/min g)	371 ± 32	408 ± 53	0.563
TVR (mmHg min/μL) $\times 10^{-3}$	5.0 ± 0.6	6.3 ± 0.5	0.118
Compliance (μL/mmHg)	0.42 ± 0.06	0.36 ± 0.03	0.326
HR (beats/min)	544 ± 15	479 ± 33	0.104
RV and pulmonary circulation			
Systolic pressure (mmHg)	21 ± 1	21 ± 2	0.963
τ (ms)	6 ± 1	9 ± 2	0.207
EF (%)	54 ± 6	43 ± 6	0.219
CI (μL/min g)	373 ± 60	332 ± 46	0.601
TVR (mmHg min/μL) $\times 10^{-3}$	2.3 ± 0.5	3.1 ± 0.5	0.319
Compliance (μL/mmHg)	0.95 ± 0.21	0.80 ± 0.16	0.606
HR (beats/min)	538 ± 8	458 ± 35	0.062
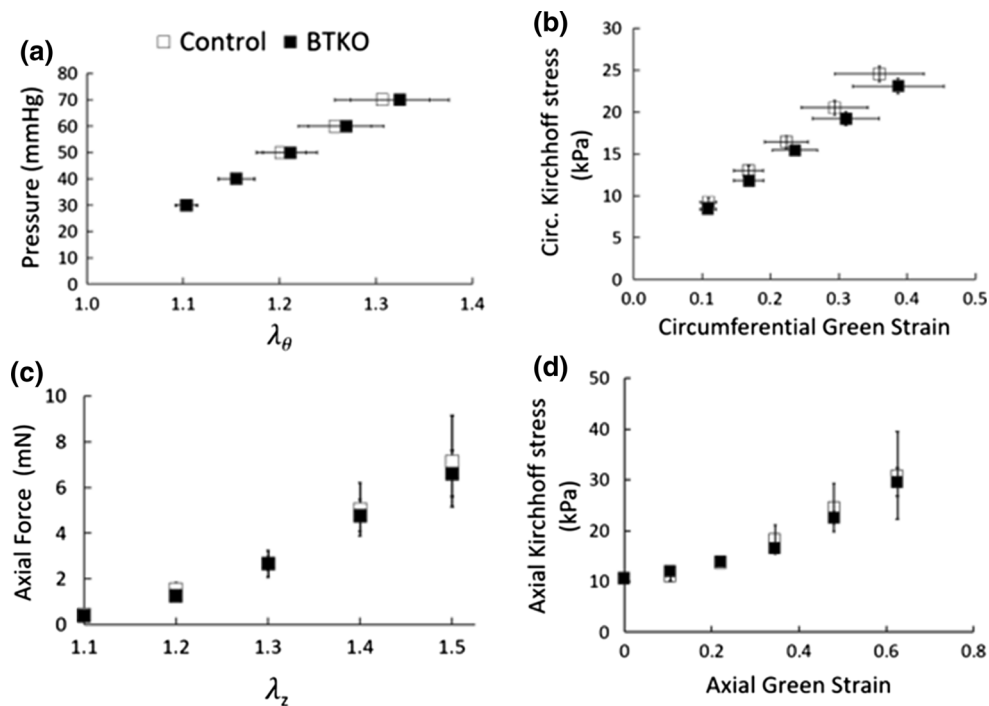
FIGURE 4. (a) Pressure-circumferential stretch values using data from the estimated *in vivo* range (30-70 mmHg). Both the control and BT^{KO} data in this range exhibit a high degree of linearity ($R^2 > 0.9$). (b) Circumferential stress–strain values using data from the estimated *in vivo* range. The moduli determined from the slope of this curve were not significantly different between control and BT^{KO} mice (see Tables 2, S5). (c) Axial force-stretch values and (d) axial stress–strain values for control and BT^{KO} mice. The moduli determined from the slope of this curve were not significantly different between control and BT^{KO} mice (see Tables 2, S5). Sample size = 14.

TABLE 2. Experimental metrics of arterial stiffness in control and BT^{KO} mice.

|	Control	BT^{KO}	*p*-value
Circumferential properties			
Elastic modulus (kPa)	76 ± 18	79 ± 21	0.900
Structural stiffness (kPa)	32 ± 7	34 ± 9	0.813
Axial properties			
Elastic modulus (kPa)	24 ± 5	30 ± 3	0.365
Structural stiffness (kPa)	8 ± 3	12 ± 2	0.256

relative drop in cardiac muscle mass (Fig. 3a–3c). Our results indicate that cardiovascular function and structure are preserved even though (i) *Bmp1* was excised in the heart (Fig. 2a), (ii) reduced procollagen and pro-biglycan processing by cardiac fibroblasts in the BT^{KO} hearts was observed (Figs. 2b and 2c), and (iii) maladaptive effects in other tissues have been reported due to *Bmp1* and *Tll1*-ablation.[33,34,52]

The preservation of cardiovascular tissue function in contrast to other tissues may be attributed to partial functional compensation by other extracellular proteinases. Similar to the functional redundancy between *Bmp1*- and *Tll1*-derived protein products,[8,34] we speculate that protein products from the related gene *Tll2* may be capable of, to some extent, functionally substituting for *Bmp1* and *Tll1*-derived protein products in adult cardiovascular tissues. Regardless of the compensatory mechanism, it appears to be inactive embryonically, since mice homozygous null for *Tll1* had significant cardiovascular defects and were embryonically lethal.[8,41] The ability of *Tll2*-derived protein products to compensate for absent *Bmp1*- and *Tll1*-derived protein products warrants further investigation. Other possible compensators for lost BTP function are the more distantly related extracellular meprin metalloproteinases, which have recently been implicated in procollagen biosynthetic processing.[38]

The absence of BT^{KO} cardiovascular dysfunction may also relate to a lower turnover of the collagenous ECM in cardiovascular tissues under normal, unstressed, conditions. Since aging causes tissue remodeling and increases the risk of cardiovascular disease
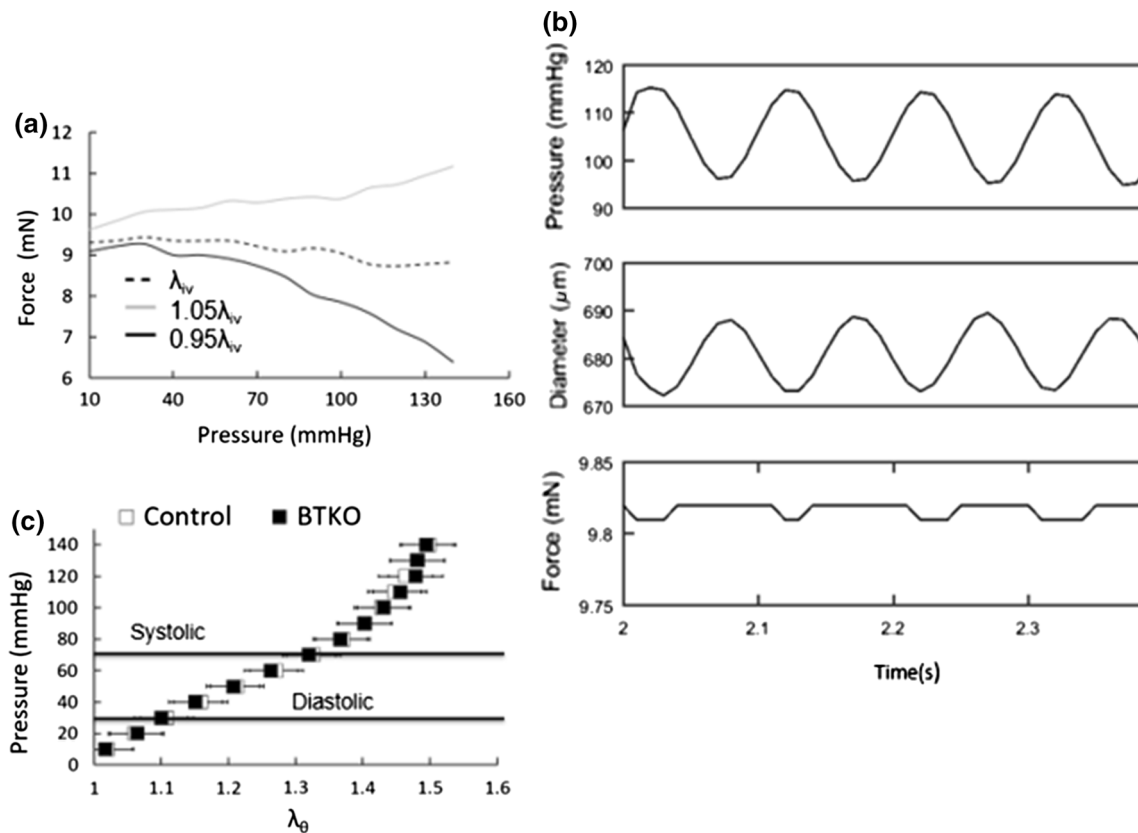
FIGURE 5. (a) Representative force-pressure relationship at multiple axial stretch values from a BT^{KO} (*in vivo,* black dotted line; 5% above *in vivo*, gray line; 5% below *in vivo*, black solid line; showing the experimental procedure to verify the *in vivo* axial stretch. (b) Representative cyclic pressure input (top panel) and diameter (middle panel) and axial force (bottom panel) responses at 10 Hz. (c) Plot of pressure-circumferential stretch to show the estimated *in vivo* pressure range used to determine mechanical properties. The mechanical response of both the control and BT^{KO} groups are similar up to pathophysiological pressures of 140 mmHg. Sample size = 14.

development,[10] we measured function in ten additional female mice at several time points (26, 30, and 34 weeks old) until they were approximately twice as old as the other mice studied here and in previous reports. However, our data in female mice up to 34 weeks of age suggest preserved cardiovascular function despite a continued reduction in body weight compared to controls (Fig. S1 Table S4).

Administration of tamoxifen may have provided some degree of a systematic protection for the cardiovascular system. Experimentally, tamoxifen administration has attenuated dilation in abdominal aortic aneurysms, reduced LV hypertrophy secondary to lower blood pressure, and decreased accumulation of collagen in the LV due to abdominal aortic constriction and isoproterenol treatment.[24,37] However, other experimental studies report tamoxifen administration had negligible or detrimental effects on the vasculature and ventricles. Specifically, blood pressure and heart rate were unaffected due to tamoxifen administration.[32] In contrast, tamoxifen administra-

tion impaired vasorelaxation in rats and adversely affected cardiac myocyte contraction and relaxation in mice.[2,32] Clinically, results from tamoxifen administration have been limited to studies of post-menopausal women, and conflicting results have been reported.[7,13] The reason for these conflicting results may be differences in species, age, dosage amounts, or chronic versus acute administration.

Body weight and cardiac muscle phenotypes observed here are consistent with previous reports from BT^{KO} mice. The reduced weight gain in BT^{KO} mice (Fig. 3a) was consistent with phenotypes reported previously.[34] The shorter tibia length (Fig. 3d) is comparable to the shorter femur found previously, and these results are indicative of the impaired skeletal growth and shorter overall mouse length.[34] Here, the reduction in cardiac muscle mass and its proportional reduction to body weight (Figs. 3b and 3c) is comparable to the reduced skeletal muscle mass reported previously.[34] It is unknown if the reduction in skeletal muscle mass found previously was associated with
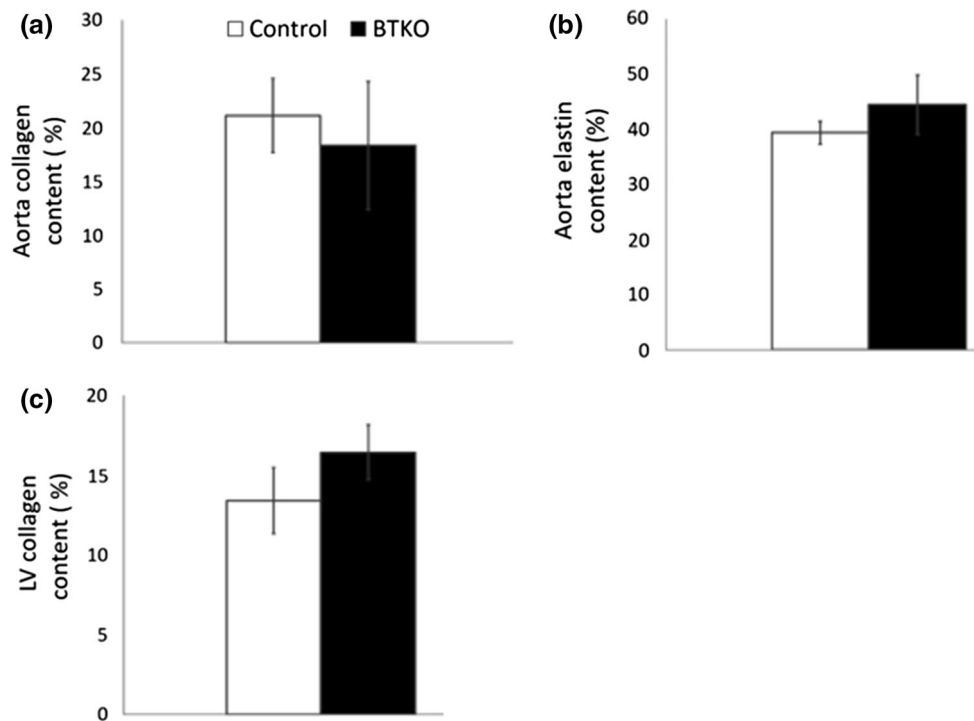
FIGURE 6. Comparison between (a) aorta collagen content, (b) aorta elastin content, and (c) LV collagen content in control and BT^{KO} mice. Sample size = 8.

impaired skeletal muscle function. Based on our findings of maintained relative cardiac muscle mass and maintained cardiac function, we speculate that the BT^{KO} mice have maintained skeletal muscle function based on maintained relative skeletal muscle mass.

Due to vessel retraction upon excision, arteries were stretched axially *ex vivo* to approximate the *in vivo* stretch. Axial stretch is reduced in response to increased loading,[11,46] so we ensured that all vessels from each group were tested at the *in vivo* axial stretch to prevent axial stretch contributing to circumferential stiffness.[26] Since pressure and afterload did not increase in BT^{KO} mice (Tables 1, S2), we expected the *in vivo* axial stretch to be preserved in BT^{KO} mice. All descending thoracic aortas were found to have an approximate *in vivo* axial stretch between 1.4 and 1.6, which is within the range of previously reported axial stretch values (1.3–1.8) from the systemic vasculature of mice.[4,11,48] A representative force-pressure relationship at multiple axial stretches for one DTA illustrates the method used to obtain λ_{iv} (Fig. 5a) as shown previously.[15] Testing at the *in vivo* axial stretch is energetically advantageous since the artery will theoretically do no axial work during a cyclic inflation. Here, we show this experimentally as evident from minimal changes in axial force during dynamic sinusoidal pressure cycles at λ_{iv} (Fig. 5b).

Most parameters used to quantify arterial stiffness are linear approximations of non-linear characteristics in non-physiological conditions. Here we examined multiple moduli in a pressure range encompassing physiological and pathological conditions using *ex vivo* loading. Catheterization of the aortic arch revealed systemic blood pressures in the range of ~ 30–70 mmHg (Table 1). While these pressures are lower than commonly reported,[6,12] the pressure-circumferential stretch data illustrate that this range encompasses the transition region for both groups in which elastin and collagen dominate load-bearing in the low- and high-stretch regions, respectively (Fig. 5c). Mechanical data in the estimated *in vivo* pressure range (data between the Systolic and Diastolic lines in Fig. 5c and data illustrated in Fig. 4a) had a very strong positive linear fit ($R^2 > 0.9$ for control and BT^{KO} mice). Using the same *in vivo* range to convert pressure to stress and stretch to strain, the circumferential stress–strain curve also had a very strong positive linear fit ($R^2 > 0.9$ for control and BT^{KO} mice; Fig. 4b), resulting in similar low-strain, high-strain, and total-strain moduli (Tables 2, S5). Above this pressure range, the circumferential mechanical behavior between genotypes was also similar (Fig. 5c). The axial force-stretch and corresponding axial stress–strain data exhibited non-linear behavior (Figs. 4c and 4d),

and the moduli values determined from the axial stress–strain curve were not significantly different between the control and BT^{KO} mice (Tables 2, S5).

Systemic arterial stiffness has long been associated with elevated pressures, so we expected preserved vascular compliance between control and BT^{KO} mice based on comparable systolic and pulse pressures (Table 1). From static mechanical tests, we observed comparable metrics of arterial stiffness in the circumferential and axial directions (Tables 2, S5). The DTA was stiffer in the circumferential compared to the axial direction as expected from previous studies.[21,45] From dynamic mechanical tests, we observed comparable dynamic modulus and arterial damping values between the two groups (Table S5), indicating that arterial conduit and buffering functions were unimpaired due to *Bmp1* and *Tll1* ablation. Preserved arterial and ventricular compliance were expected based on the comparable ECM protein content between groups (Fig. 6). The ventricular afterload E$_a$ is dependent on both vascular compliance and resistance; the preservation of E$_a$ in BT^{KO} mice is consistent with the *ex vivo* arterial mechanical testing results (Tables 2, S5).

Limitations

We assessed the regulation of arterial stiffness by collagen proteins, but vascular smooth muscle cells (SMC) also regulate arterial stiffness. We tested mechanical properties in the absence of SMC activation using Mg^{2+}/Ca^{2+}-free physiological buffer solution to distinguish contributions of collagen and elastin to mechanical properties from those of active SMC. We combined the male and female results to isolate the effect of the double gene knockout since we found similar trends in cardiovascular structure and function, and results from skeletal tissues were previously shown to be similar between the two sexes.[34] Tamoxifen may impart beneficial effects on the cardiovascular system, but tamoxifen administration was necessary for comparison between control and BT^{KO} groups. Only one control group was used; administering tamoxifen to mice without the floxed genes would have been a second appropriate comparison group. The mechanical analysis used here assumes the arteries are single layered homogenous tissues. Finally, we investigated cardiovascular function in these mice without an external stressor (i.e. hypoxia, angiotensin infusion, *etc.*) since abnormalities were found in other tissues from the knockout alone. The combination of a stressor with ablation of BMP1-related proteinases could reveal clinically relevant pathophysiology and is an important direction for future work.

CONCLUSION

In summary, despite the importance of fibrillar collagens to cardiovascular tissue function, cardiovascular function and structure are preserved after induced ablation of genes encoding for BMP1-related proteinases. This finding, together with the finding of decreased procollagen processing by BT^{KO} cardiac fibroblasts, suggests that there is an as-yet unidentified post-natal compensatory mechanism in cardiovascular tissues due to *Bmp1* and *Tll1*-ablation.

ELECTRONIC SUPPLEMENTARY MATERIAL

The online version of this article (https://doi.org/10.1007/s12195-018-0534-y) contains supplementary material, which is available to authorized users.

CONFLICT OF INTEREST

Mark Golob, Dawiyat Massoudi, Diana Tabima, James Johnston, Gregory Wolf, Timothy Hacker, Daniel Greenspan, and Naomi Chesler declare they have no conflicts of interest.

ETHICAL APPROVAL

This article does not contain any studies with human participants performed by any of the authors. All applicable international, national, and/or institutional guidelines for the care and use of animals were followed.

REFERENCES

[1] Amin, M., V. P. Le, and J. E. Wagenseil. Mechanical testing of mouse carotid arteries: From newborn to adult. *J Vis Exp* 2012. https://doi.org/10.3791/3733.

[2] Asp, M. L., J. J. Martindale, and J. M. Metzger. Direct, differential effects of tamoxifen, 4-hydroxytamoxifen, and raloxifene on cardiac myocyte contractility and calcium handling. *PLoS ONE* 8:e78768, 2013.

[3] Baicu, C. F., J. D. Stroud, V. A. Livesay, E. Hapke, J. Holder, F. G. Spinale, and M. R. Zile. Changes in extracellular collagen matrix alter myocardial systolic performance. *Am. J. Physiol. Heart Circ. Physiol.* 284:H122–H132, 2003.

[4] Bersi, M. R., J. Ferruzzi, J. F. Eberth, R. L. Gleason, Jr, and J. D. Humphrey. Consistent biomechanical phenotyping of common carotid arteries from seven genetic, pharmacological, and surgical mouse models. *Ann. Biomed. Eng.* 42:1207–1223, 2014.

[5] Brody, M. J., T. A. Hacker, J. R. Patel, L. Feng, J. Sadoshima, S. G. Tevosian, R. C. Balijepalli, R. L. Moss, and Y. Lee. Ablation of the cardiac-specific gene leucine-rich repeat containing 10 (lrrc10) results in dilated cardiomyopathy. *PLoS One* 7:e51621, 2012.

[6] Carta, L., J. E. Wagenseil, R. H. Knutsen, B. Mariko, G. Faury, E. C. Davis, B. Starcher, R. P. Mecham, and F. Ramirez. Discrete contributions of elastic fiber components to arterial development and mechanical compliance. *Arterioscler. Thromb. Vasc. Biol.* 29:2083–2089, 2009.

[7] Christodoulakos, G. E., I. V. Lambrinoudaki, and D. C. Botsis. The cardiovascular effects of selective estrogen receptor modulators. *Ann. N. Y. Acad. Sci.* 1092:374–384, 2006.

[8] Clark, T. G., S. J. Conway, I. C. Scott, P. A. Labosky, G. Winnier, J. Bundy, B. L. Hogan, and D. S. Greenspan. The mammalian tolloid-like 1 gene, tll1, is necessary for normal septation and positioning of the heart. *Development* 126:2631–2642, 1999.

[9] D'Armiento, J. Matrix metalloproteinase disruption of the extracellular matrix and cardiac dysfunction. *Trends Cardiovasc. Med.* 12:97–101, 2002.

[10] Denker, M. G., and D. L. Cohen. What is an appropriate blood pressure goal for the elderly: review of recent studies and practical recommendations. *Clin. Interv. Aging* 8:1505–1517, 2013.

[11] Eberth, J. F., V. C. Gresham, A. K. Reddy, N. Popovic, E. Wilson, and J. D. Humphrey. Importance of pulsatility in hypertensive carotid artery growth and remodeling. *J. Hypertens.* 27:2010–2021, 2009.

[12] Eberth, J. F., N. Popovic, V. C. Gresham, E. Wilson, and J. D. Humphrey. Time course of carotid artery growth and remodeling in response to altered pulsatility. *Am. J. Physiol. Heart Circ. Physiol.* 299:H1875–H1883, 2010.

[13] Esteva, F. J., and G. N. Hortobagyi. Comparative assessment of lipid effects of endocrine therapy for breast cancer: implications for cardiovascular disease prevention in postmenopausal women. *Breast* 15:301–312, 2006.

[14] Faury, G., G. M. Maher, D. Y. Li, M. T. Keating, R. P. Mecham, and W. A. Boyle. Relation between outer and luminal diameter in cannulated arteries. *Am. J. Physiol.* 277:H1745–H1753, 1999.

[15] Ferruzzi, J., M. R. Bersi, and J. D. Humphrey. Biomechanical phenotyping of central arteries in health and disease: advantages of and methods for murine models. *Ann. Biomed. Eng.* 41:1311–1330, 2013.

[16] Fisher, L. W., J. T. Stubbs, 3rd, and M. F. Young. Antisera and cdna probes to human and certain animal model bone matrix noncollagenous proteins. *Acta Orthop. Scand. Suppl.* 266:61–65, 1995.

[17] Fomovsky, G. M., S. Thomopoulos, and J. W. Holmes. Contribution of extracellular matrix to the mechanical properties of the heart. *J. Mol. Cell. Cardiol.* 48:490–496, 2010.

[18] Gaballa, M. A., C. T. Jacob, T. E. Raya, J. Liu, B. Simon, and S. Goldman. Large artery remodeling during aging: biaxial passive and active stiffness. *Hypertension* 32:437–443, 1998.

[19] Ge, G., and D. S. Greenspan. Developmental roles of the bmp1/tld metalloproteinases. *Birth Defects Res. C* 78:47–68, 2006.

[20] Gleason, R. L., S. P. Gray, E. Wilson, and J. D. Humphrey. A multiaxial computer-controlled organ culture and biomechanical device for mouse carotid arteries. *J. Biomech. Eng.* 126:787, 2004.

[21] Golob, M. J., D. M. Tabima, G. D. Wolf, J. L. Johnston, O. Forouzan, A. M. Mulchrone, H. B. Kellihan, M. L. Bates, and N. C. Chesler. Pulmonary arterial strain- and remodeling-induced stiffening are differentiated in a chronic model of pulmonary hypertension. *J. Biomech.* 55:92–98, 2017.

[22] Golob, M. J., L. Tian, Z. Wang, T. A. Zimmerman, C. A. Caneba, T. A. Hacker, G. Song, and N. C. Chesler. Mitochondria DNA mutations cause sex-dependent development of hypertension and alterations in cardiovascular function. *J. Biomech.* 48:405–412, 2015.

[23] Golob, M. J., Z. Wang, A. J. Prostrollo, T. A. Hacker, and N. C. Chesler. Limiting collagen turnover via collagenase-resistance attenuates right ventricular dysfunction and fibrosis in pulmonary arterial hypertension. *Physiol Rep* 2016. https://doi.org/10.14814/phy2.12815.

[24] Grigoryants, V., K. K. Hannawa, C. G. Pearce, I. Sinha, K. J. Roelofs, G. Ailawadi, K. B. Deatrick, D. T. Woodrum, B. S. Cho, P. K. Henke, J. C. Stanley, M. J. Eagleton, and G. R. Upchurch. Tamoxifen up-regulates catalase production, inhibits vessel wall neutrophil infiltration, and attenuates development of experimental abdominal aortic aneurysms. *J. Vasc. Surg.* 41:108–114, 2005.

[25] Hopkins, D. R., S. Keles, and D. S. Greenspan. The bone morphogenetic protein 1/tolloid-like metalloproteinases. *Matrix Biol.* 26:508–523, 2007.

[26] Humphrey, J. D. Cardiovascular solid mechanics: cells, tissues, and organs. Berlin: Springer Science & Business Media, 2013.

[27] Kobayashi, K., M. Luo, Y. Zhang, D. C. Wilkes, G. Ge, T. Grieskamp, C. Yamada, T. C. Liu, G. Huang, C. T. Basson, A. Kispert, D. S. Greenspan, and T. N. Sato. Secreted frizzled-related protein 2 is a procollagen c proteinase enhancer with a role in fibrosis associated with myocardial infarction. *Nat. Cell Biol.* 11:46–55, 2009.

[28] Kobs, R. W., and N. C. Chesler. The mechanobiology of pulmonary vascular remodeling in the congenital absence of enos. *Biomech. Model Mechanobiol.* 5:217–225, 2006.

[29] Kobs, R. W., N. E. Muvarak, J. C. Eickhoff, and N. C. Chesler. Linked mechanical and biological aspects of remodeling in mouse pulmonary arteries with hypoxia-induced hypertension. *Am. J. Physiol. Heart Circ. Physiol.* 288:H1209–H1217, 2005.

[30] Liu, A., L. Tian, M. Golob, J. C. Eickhoff, M. Boston, and N. C. Chesler. 17beta-estradiol attenuates conduit pul-

monary artery mechanical property changes with pulmonary arterial hypertension. *Hypertension* 66:1082–1088, 2015.

[31]London, G. M., S. J. Marchais, A. P. Guerin, and B. Pannier. Arterial stiffness: pathophysiology and clinical impact. *Clin. Exp. Hypertens.* 26:689–699, 2004.

[32]Montenegro, M. F., L. R. Pessa, V. A. Gomes, Z. Desta, D. A. Flockhart, and J. E. Tanus-Santos. Assessment of vascular effects of tamoxifen and its metabolites on the rat perfused hindquarter vascular bed. *Basic Clin. Pharmacol. Toxicol.* 104:400–407, 2009.

[33]Muir, A. M., D. Massoudi, N. Nguyen, D. R. Keene, S. J. Lee, D. E. Birk, J. M. Davidson, M. P. Marinkovich, and D. S. Greenspan. Bmp1-like proteinases are essential to the structure and wound healing of skin. *Matrix Biol.* 56:114–131, 2016.

[34]Muir, A. M., Y. Ren, D. H. Butz, N. A. Davis, R. D. Blank, D. E. Birk, S. J. Lee, D. Rowe, J. Q. Feng, and D. S. Greenspan. Induced ablation of bmp1 and tll1 produces osteogenesis imperfecta in mice. *Hum. Mol. Genet.* 23:3085–3101, 2014.

[35]Nimni, M. Collagen in cardiovascular tissuesCardiovascular biomaterials, New York: Springer, pp. 81–141, 1992.

[36]Ooi, C. Y., Z. Wang, D. M. Tabima, J. C. Eickhoff, and N. C. Chesler. The role of collagen in extralobar pulmonary artery stiffening in response to hypoxia-induced pulmonary hypertension. *Am. J. Physiol. Heart Circ. Physiol.* 299:H1823–H1831, 2010.

[37]Patel, B. M., and V. J. Desai. Beneficial role of tamoxifen in experimentally induced cardiac hypertrophy. *Pharmacol. Rep.* 66:264–272, 2014.

[38]Prox, J., P. Arnold, and C. Becker-Pauly. Meprin alpha and meprin beta: procollagen proteinases in health and disease. *Matrix Biol.* 44–46:7–13, 2015.

[39]Rodriguez-Feo, J. A., J. P. Sluijter, D. P. de Kleijn, and G. Pasterkamp. Modulation of collagen turnover in cardiovascular disease. *Curr. Pharm. Des.* 11:2501–2514, 2005.

[40]Scott, I. C., Y. Imamura, W. N. Pappano, J. M. Troedel, A. D. Recklies, P. J. Roughley, and D. S. Greenspan. Bone morphogenetic protein-1 processes probiglycan. *J. Biol. Chem.* 275:30504–30511, 2000.

[41]Suzuki, N., P. A. Labosky, Y. Furuta, L. Hargett, R. Dunn, A. B. Fogo, K. Takahara, D. M. Peters, D. S. Greenspan, and B. L. Hogan. Failure of ventral body wall closure in mouse embryos lacking a procollagen c-proteinase encoded by bmp1, a mammalian gene related to drosophila tolloid. *Development* 122:3587–3595, 1996.

[42]Tabima, D. M., and N. C. Chesler. The effects of vasoactivity and hypoxic pulmonary hypertension on extralobar pulmonary artery biomechanics. *J. Biomech.* 43:1864–1869, 2010.

[43]Tabima, D. M., T. A. Hacker, and N. C. Chesler. Measuring right ventricular function in the normal and hypertensive mouse hearts using admittance-derived pressure-volume loops. *Am. J. Physiol. Heart Circ. Physiol.* 299:H2069–2075, 2010.

[44]Takahara, K., G. E. Lyons, and D. S. Greenspan. Bone morphogenetic protein-1 and a mammalian tolloid homologue (mtld) are encoded by alternatively spliced transcripts which are differentially expressed in some tissues. *J. Biol. Chem.* 269:32572–32578, 1994.

[45]Tian, L., J. Henningsen, M. R. Salick, W. C. Crone, M. Gunderson, S. H. Dailey, and N. C. Chesler. Stretch calculated from grip distance accurately approximates mid-specimen stretch in large elastic arteries in uniaxial tensile tests. *J Mech. Behav. Biomed. Mater.* 47:107–113, 2015.

[46]Vaishnav, R. N., J. Vossoughi, D. J. Patel, L. N. Cothran, B. R. Coleman, and E. L. Ison-Franklin. Effect of hypertension on elasticity and geometry of aortic tissue from dogs. *J. Biomech. Eng.* 112:70–74, 1990.

[47]Wagenseil, J. E., and R. P. Mecham. Elastin in large artery stiffness and hypertension. *J. Cardiovasc. Transl. Res.* 5:264–273, 2012.

[48]Wagenseil, J. E., N. L. Nerurkar, R. H. Knutsen, R. J. Okamoto, D. Y. Li, and R. P. Mecham. Effects of elastin haploinsufficiency on the mechanical behavior of mouse arteries. *Am. J. Physiol. Heart Circ. Physiol.* 289:H1209–H1217, 2005.

[49]Wang, Z., and N. C. Chesler. Role of collagen content and cross-linking in large pulmonary arterial stiffening after chronic hypoxia. *Biomech. Model Mechanobiol.* 11:279–289, 2012.

[50]Wang, Z., R. S. Lakes, J. C. Eickhoff, and N. C. Chesler. Effects of collagen deposition on passive and active mechanical properties of large pulmonary arteries in hypoxic pulmonary hypertension. *Biomech. Model Mechanobiol.* 12:1115–1125, 2013.

[51]Wang, Z., R. S. Lakes, M. Golob, J. C. Eickhoff, and N. C. Chesler. Changes in large pulmonary arterial viscoelasticity in chronic pulmonary hypertension. *PLoS One* 8:e78569, 2013.

[52]Wang, J., D. Massoudi, Y. Ren, A. M. Muir, S. E. Harris, D. S. Greenspan, and J. Q. Feng. Bmp1 and tll1 are required for maintaining periodontal homeostasis. *J. Dent. Res.* 96:578–585, 2017.

[53]Wang, Z., M.J. Golob, and N.C. Chesler, *Viscoelastic properties of cardiovascular tissues*, in *Viscoelastic and viscoplastic materials*. 2016, InTech.